

## NON-LINEAR ANALYSIS OF CAPACITOR MOTOR USING THE ANISOTROPIC FIELD MODEL

Gheorghe MADESCU\*, Marius BIRIESCU\*\* Marțian MOȚ\*, Lucian OCOLIȘAN\*

\* Romanian Academy – Timisoara Branch, B.dul M. Viteazul nr. 24, 300223 – Timisoara, Romania,  
E-mail: gmadescu@d109lin.utt.ro

\*\* Technical University of Timișoara, Faculty of Electrical Engineering, B.dul V. Pârvan nr.2, 300223 – Timisoara, Romania;  
E-mail: biri@d109lin.utt.ro

The present paper introduces a combined circuit-field model of a capacitor motor with cage rotor using both the two-axes and anisotropic field model. This approach represents a simple way to compute more precisely the nonlinear magnetization characteristic of split-phase motors. The calculated magnetization characteristic is validated by tests on no load (with and without rotor cage).

*Key words:* capacitor motor, circuit-field model, cross-saturation effect.

### 1. INTRODUCTION

The split-phase motors (with capacitor or resistance) are usually low power machines and are widely used for both industrial and home appliances.

For the analysis of this motors have been extensively developed a wide variety of analytical models [1, 2, 3, 4] based on rotating-field theory or two-axes theory. This circuit models usually assume that the magnetic core have infinity (or constant) permeability. In reality there is a clear nonlinear interdependence between the currents and the impedances (or fluxes). Many tests shows that the iron saturation must be taken into account in the motor model otherwise there is a discordance between the computed and measured values. In [5], the iron saturation is taken into account by computing the positive-sequence impedance by an iterative procedure.

Because of high levels of main flux path saturation it is necessary to implicate in the problem a field model. The finite element models (FEM) are commonly used for induction machine analysis, but prohibitive computing time required by FEM limits their use to special cases. In [6] is explained how the finite element techniques can be used when iron saturation is included.

In this paper a combined circuit-field model of capacitor motor with cage rotor is presented. The field model is interfaced with the circuit equations (two-axes model) such that to compute more precisely the nonlinear magnetization characteristic (induced voltage versus resultant magnetizing current).

### 2. THE FIELD MODEL

In the magnetic field problem is used the anisotropic (orthotropic) model presented and complete validated by test on no load and on load for several three-phase induction motors [7].

The cross section of the induction machine is divided into five circular layers (Fig.1). The both stator and rotor slotting layer are homogenized and becomes anisotropic domain, with distinct magnetic permeabilities  $\mu_r$  and  $\mu_\theta$  along the radial and tangential directions.

This multilayers homogeneous model leads, as a consequence, to the analytical solution of the field differential equations. Finally, the magnetic potential expressions for the five layers are:

$$\begin{aligned}
 A_1(r, \theta) &= (g_1 \cdot r^{p_1} + h_1 \cdot r^{-p_1}) \sin(p_1 \theta); & a < r < b \\
 A_3(r, \theta) &= (g_3 \cdot r^{p_1} + h_3 \cdot r^{-p_1}) \sin(p_1 \theta); & c < r < d \\
 A_5(r, \theta) &= (g_5 \cdot r^{p_1} + h_5 \cdot r^{-p_1}) \sin(p_1 \theta); & e < r < f \\
 A_2(r, \theta) &= (g_2 \cdot r^{p_1 \alpha_2} + h_2 \cdot r^{-p_1 \alpha_2} + k_2 \cdot r^2) \sin(p_1 \theta); & b < r < c \\
 A_4(r, \theta) &= (g_4 \cdot r^{p_1 \alpha_4} + h_4 \cdot r^{-p_1 \alpha_4} + k_4 \cdot r^2) \sin(p_1 \theta); & d < r < e
 \end{aligned} \tag{1}$$

with

$$k_2 = + \frac{\mu_{r2} \cdot \mu_{\theta 2}}{4\mu_{r2} - p_1^2 \mu_{\theta 2}} \cdot J_{m2}; \quad k_4 = - \frac{\mu_{r4} \cdot \mu_{\theta 4}}{4\mu_{r4} - p_1^2 \mu_{\theta 4}} \cdot J_{m4}. \tag{2}$$

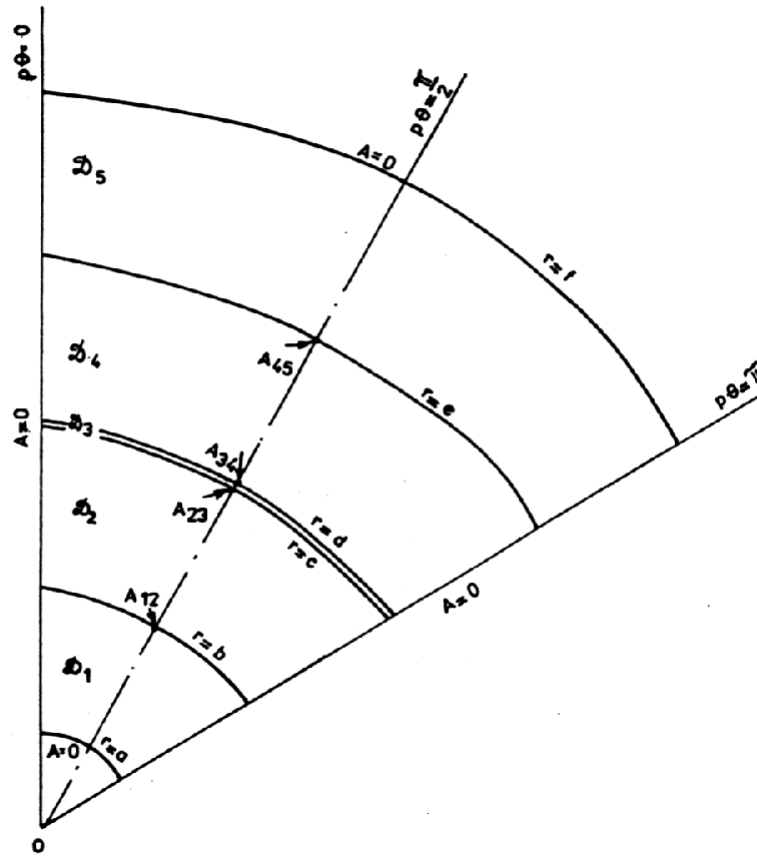


Fig. 1. The IM cross-section divided into five domains

The magnitudes of the sinusoidal distribution of the stator and rotor equivalent current density ( $J_{m2}$ ,  $J_{m4}$ ) are related to the reactive stator and rotor phase currents ( $I_{1r}$  and  $I_{2r}'$ ) by the expression (for the single-phase motor with cage rotor):

$$J_{m2} = \frac{4\sqrt{2}}{\pi} \cdot \frac{1}{c^2 - b^2} \cdot W_1 k_{w1} I_{2r}'; \quad J_{m4} = \frac{4\sqrt{2}}{\pi} \cdot \frac{1}{e^2 - d^2} \cdot W_1 k_{w1} I_{1r}. \tag{3}$$

The main pole-flux-linkage  $\Phi_m$  is obtained through the line integral of  $A_3$  around a pole contour  $\Gamma$ :

$$\Phi_m = \oint_{\Gamma} \overline{A_3} \cdot d\overline{l} = 2 L_1 (g_3 d^{p_1} + h_3 d^{-p_1}) \quad (4)$$

Finally, the e.m.f.  $U_e$  (RMS value) is:

$$U_e = \pi\sqrt{2} \cdot f_1 W_1 k_{w1} \Phi_m \quad (5)$$

The integration constants ( $g_i$ ,  $h_i$ ) and the iterative computer program was presented in [7]. At every cycle of computation each equivalent permeability is changed according to a specific relation, so that a very good convergence rate is obtained.

The program gives (step by step) the nonlinear magnetization characteristic  $U_e(I_m)$  where  $I_m$  is the total magnetizing current (stator and rotor current).

Some other anisotropic models was presented in references [8, 9, 10].

### 3. THE TWO-AXES CIRCUIT MODEL

The most of split-phase induction motors have two stator windings in space electric quadrature. Because of this structure two-axes model (dq-model) is extensively used to analyze the motor (Fig. 2). The auxiliary windings (B) have inductive or capacitive characteristic and serve to start the motor. The rotor cage is equivalent with two rotor windings corresponding to the both d and q axes.

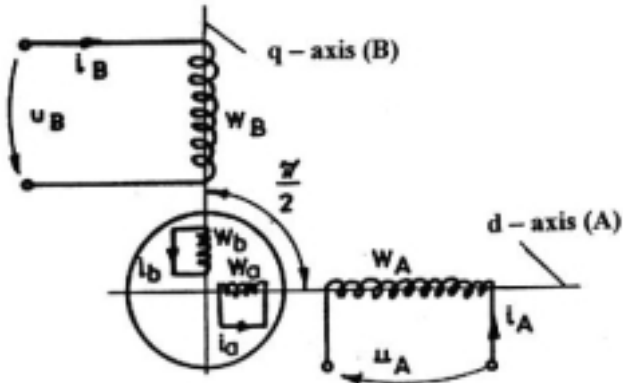


Fig. 2. The dq-model of the machine

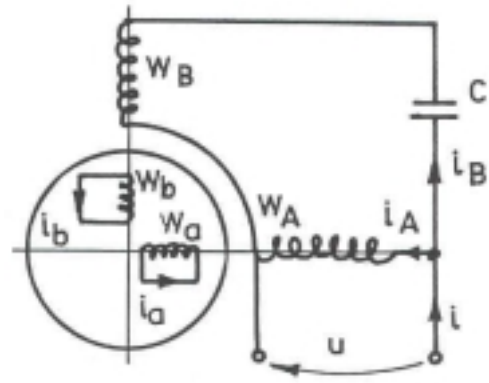


Fig. 3. The circuit diagram of the capacitor motor

The used mathematical model [11, 12] is:

$$\begin{bmatrix} u_A \\ u_B \\ 0 \\ 0 \end{bmatrix} = \begin{bmatrix} R_A + pL_A & 0 & 0 & pM_A \\ 0 & R_B + pL_B & pM_B & 0 \\ \omega_r M_A & pM_B & R_b + pL_b & \omega_r L_a \\ pM_A & -\omega_r M_B & -\omega_r L_b & R_a + pL_a \end{bmatrix} \begin{bmatrix} i_A \\ i_B \\ i_b \\ i_a \end{bmatrix} \quad (6)$$

This model is developed for the sinusoidal operation so that it can be coupled with the above field model.

Finally, the following complex form of equation is obtained:

$$\begin{aligned} \underline{U}_A &= \underline{Z}_A \underline{I}_A - \underline{U}_{eA}; & \underline{U}_B &= \underline{Z}_B \underline{I}_B - \underline{U}_{eB} \\ 0 &= j(1-s)k_{BA} \underline{U}_{eA} - \underline{U}_{eB} + \underline{Z}'_b \underline{I}'_b + (1-s)k_{BA} X'_{\sigma a} \underline{I}'_a \\ 0 &= -j(1-s)\underline{U}_{eB} - k_{BA} \underline{U}_{eA} + k_{BA} \underline{Z}'_a \underline{I}'_a - (1-s)X'_{\sigma b} \underline{I}'_b \end{aligned} \quad (7)$$

where:

$$\underline{U}_{eA} = -j X_{mA} (\underline{I}_A + \underline{I}'_a); \quad \underline{U}_{eB} = -j X_{mB} (\underline{I}_B + \underline{I}'_b); \quad k_{BA} = \frac{W_B k_{WB}}{W_A k_{WA}}. \quad (8)$$

In the case of capacitor motor (fig.3) two supplementary equations is adding:

$$\underline{I} = \underline{I}_A + \underline{I}_B; \quad \underline{U}_A = \underline{U}_B + \underline{Z}_C \underline{I}_B \quad (9)$$

where  $\underline{Z}_C = -j X_C = -j \frac{1}{\omega C}$  is the capacitor impedance.

#### 4. THE COUPLED MODEL IN THE CASE WITHOUT ROTOR CAGE

In this paragraph is presented an example for the coupling of both models mentioned above for a capacitor motor without rotor cage.

In such a motor there is two magnetization characteristics  $U_{eA}(I_{mA})$  and  $U_{eB}(I_{mB})$  corresponding to the d and q axis, with different magnetic conditions.

If the capacitor motor have not rotor cage ( $I'_a = I'_b = 0$ ) in the mathematical model remain only the stator voltage equations:

$$\underline{U}_A = \underline{Z}_A \underline{I}_A - \underline{U}_{eA}; \quad \underline{U}_B = \underline{Z}_{BC} \underline{I}_B - \underline{U}_{eB} \quad (10)$$

where  $\underline{Z}_{BC} = \underline{Z}_B + \underline{Z}_C$ .

In no-load condition (the rotor is driven from the outside at the synchronous speed), if the active components of the currents are neglected, this can be written:

$$\underline{I}_A \approx \underline{I}_{mA} = j I_{mA}; \quad \underline{I}_B \approx \underline{I}_{mB} = j I_{mB} e^{j\varphi} \quad (11)$$

where  $\varphi$  is the shift angle between the phasors  $\underline{I}_{mB}$  and  $\underline{I}_{mA}$ .

With complex variable it might be written:

$$\underline{U}_{eA} = U_{eA}; \quad \underline{U}_{eB} = U_{eB} e^{j\varphi}; \quad \underline{U}_A = U_A e^{j\beta}; \quad \underline{Z}_A = Z_A e^{j\alpha_A}; \quad \underline{Z}_{BC} = Z_{BC} e^{j\alpha_{BC}} \quad (12)$$

Replacing the terms in the equation (10) there results:

$$U_A e^{j\beta} = Z_A e^{j\alpha_A} \cdot j I_{mA} - U_{eA}; \quad U_A e^{j\beta} = Z_{BC} e^{j\alpha_{BC}} \cdot j I_{mB} e^{j\varphi} - U_{eB} e^{j\varphi} \quad (13)$$

Separating the real terms from the imaginary ones, from (13) results four real equations:

$$U_A \cos \beta = -Z_A I_{mA} \sin \alpha_A - U_{eA}; \quad U_A \sin \beta = Z_A I_{mA} \cos \alpha_A \quad (14)$$

$$U_A \cos \beta = -Z_{BC} I_{mB} \sin(\alpha_{BC} + \varphi) - U_{eB} \cos \varphi; \quad U_A \sin \beta = Z_{BC} I_{mB} \cos(\alpha_{BC} + \varphi) - U_{eB} \sin \varphi.$$

Eliminating the shift angles  $\varphi$  and  $\beta$ , we finally get:

$$U_A^2 = (U_{eA} + X_{\sigma A} I_{mA})^2 + R_A^2 I_{mA}^2; \quad U_A^2 = (U_{eB} + X_{\sigma B} I_{mB} - X_C I_{mB})^2 + R_B^2 I_{mB}^2 \quad (15)$$

When iron saturation is included, this two last equations are connected because  $U_{eA}$  and  $U_{eB}$  becomes nonlinear functions of both  $I_{mA}$  and  $I_{mB}$  magnetizing currents:  $U_{eA} = U_{eA}(I_{mA}, I_{mB})$ ,  $U_{eB} = U_{eB}(I_{mA}, I_{mB})$ .

This nonlinear function  $U_{eA}$  and  $U_{eB}$  can be calculated from the field model and assures the coupling with the circuit model.

The system (15) has only two independent variables:  $I_{mA}$ ,  $I_{mB}$ ; in order to solve this system of equations there has been elaborated an iterative numerical algorithm. This system establishes the real operation points of the machine on the both  $U_{eA}$  and  $U_{eB}$  magnetization characteristics.

In consequence, the magnetizing reactances for d and q axes are the following:

$$X_{mA} = \frac{U_{eA}(I_{mA}, I_{mB})}{I_{mA}}; \quad X_{mB} = \frac{U_{eB}(I_{mA}, I_{mB})}{I_{mB}}. \quad (16)$$

In order to test it experimentally, there has been used a 4 pole capacitor motor, with rated power 1,5 kW and stator parameters:  $R_A=2,8 \Omega$ ;  $X_{\sigma A}=7 \Omega$ ;  $k_{BA}=1,52$ ;  $R_B=6,7 \Omega$ ;  $X_{\sigma B}=11 \Omega$ .

The rotor has built up without any cage and was driven at synchronous speed. In this no-load condition, at different values of voltage  $U_A$  ( $f=50$  Hz) we have measured the currents  $I_A \approx I_{mA}$  and  $I_B \approx I_{mB}$ .

Figure 4 shows the variation of the current  $I_{mA}$  related to voltage  $U_A$  for different values of capacitor. It is interesting to see that, for same voltage  $U_A$  the magnetizing current  $I_{mA}$  is different for different values of capacitor, because the current  $I_{mB}$  produce the magnetization of both d and q axes.

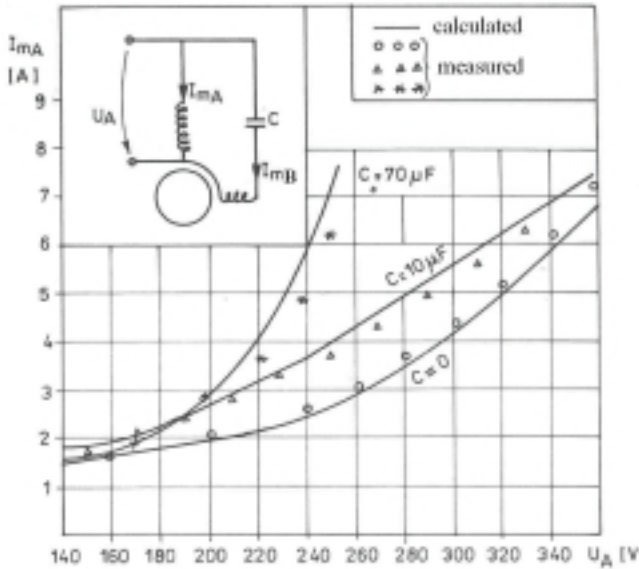


Fig. 4. The variation of the current  $I_{mA}$  versus  $U_A$  – voltage for different capacitors

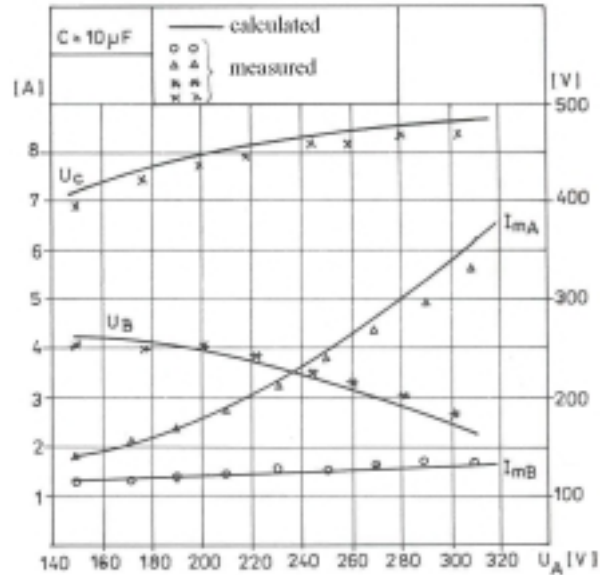


Fig. 5. The variation of the current and voltages versus  $U_A$  – voltage

There is good correlation between the computed values (according to the algorithm presented in [7]) and the measured values, even for high saturation levels.

Figure 5 present the variation of both  $I_{mA}$  and  $I_{mB}$  current, capacitor voltage ( $U_C$ ) and phase B voltage, related to voltage  $U_A$ , for constant capacitor  $C=10 \mu\text{F}$ . The experimental data are very near to the curves obtained by computing.

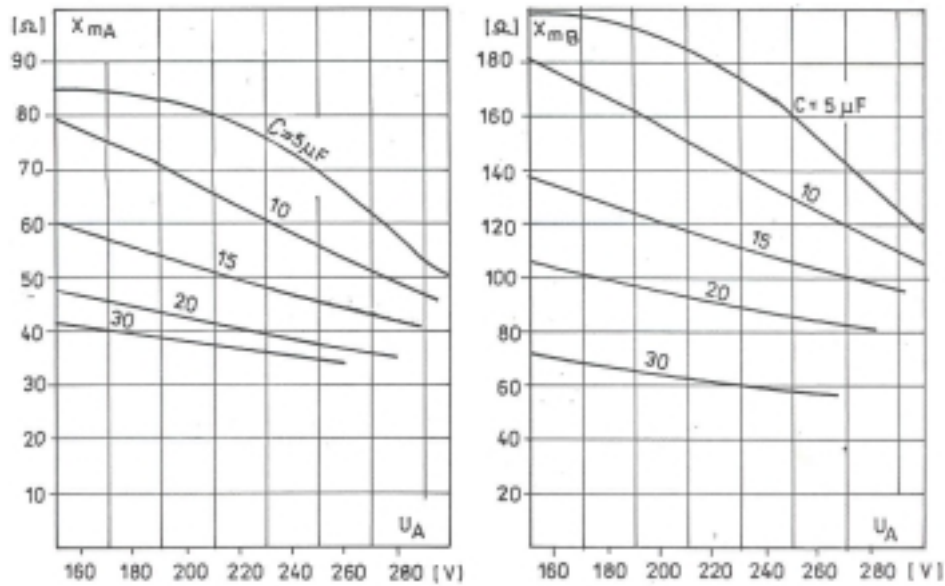


Fig. 6. The influence of the voltage ( $U_A$ ) and capacitor values on the magnetizing reactances

The calculated values of the magnetizing reactances  $X_{mA}$  and  $X_{mB}$  for different values of the voltage  $U_A$  and capacitor are represented in figure 6. It is clear that each of the magnetizing reactances have a double dependence if the saturation is taken into account.

This is so called “cross-saturation effect” that consists of dependence of the steady-state d-q axes magnetizing inductances on the currents in both axes. In other words, in saturated conditions the d and q axes are connected, from the magnetic point of view.

## 5. THE COUPLED MODEL IN THE CASE WITH ROTOR CAGE

When the capacitor motor have a squirrel cage in the rotor, even in no-load condition ( $s=0$ ), there is rotor currents and we must be considered all the equations of system (7).

By solving this system, the solutions in the final form become:

$$\underline{I}_A = \frac{\underline{U}_A - jX_{mA}\underline{I}'_a}{\underline{Z}_A + jX_{mA}}; \quad \underline{I}_B = \frac{\underline{U}_A - jX_{mB}\underline{I}'_b}{\underline{Z}_{BC} + jX_{mB}}; \quad \underline{I}'_a = \frac{T_1T_6 - T_3T_4}{T_2T_6 - T_3T_5}; \quad \underline{I}'_b = \frac{T_1T_5 - T_2T_4}{T_3T_5 - T_2T_6} \quad (17)$$

where:

$$\begin{aligned} T_1 &= \left( -\frac{k_{BA}(1-s)X_{mA}}{\underline{Z}_A + jX_{mA}} - \frac{jX_{mB}}{\underline{Z}_{BC} + jX_{mB}} \right) \underline{U}_A; \quad T_2 = k_{BA}(1-s) \left( -\frac{jX_{mA}^2}{\underline{Z}_A + jX_{mA}} + X_{mA} + X'_{\sigma a} \right) \\ T_3 &= \frac{X_{mB}^2}{\underline{Z}_{BC} + jX_{mB}} + jX_{mB} + \underline{Z}'_b; \quad T_4 = \left( -\frac{jk_{BA}X_{mA}}{\underline{Z}_A + jX_{mA}} + \frac{(1-s)X_{mB}}{\underline{Z}_{BC} + jX_{mB}} \right) \underline{U}_A \\ T_5 &= k_{BA} \left( \frac{X_{mA}^2}{\underline{Z}_A + jX_{mA}} + jX_{mA} + \underline{Z}'_a \right); \quad T_6 = (1-s) \left( \frac{jX_{mB}^2}{\underline{Z}_{BC} + jX_{mB}} - X_{mB} - X'_{\sigma b} \right) \end{aligned} \quad (18)$$

and:

$$\underline{Z}'_a = R'_a + jX'_{\sigma a}; \quad \underline{Z}'_b = R'_b + jX'_{\sigma b} = k_{BA}^2 \underline{Z}'_a. \quad (19)$$

In this relations are calculated at first the magnetizing reactances  $X_{mA}$  and  $X_{mB}$  like in paragraph 4 and next the currents with the relations (17).

Following this way was determinate the no-load current of the same motor having a rotor with squirrel cage ( $R'_a = 2,9 \Omega$ ;  $X'_{\sigma a} = 2,1 \Omega$ ), for fixed capacitor  $C=10 \mu\text{F}$  and for different values of supply voltage  $U_A$ .

The computed and experimental data was presented in figure 7; there is a good correlation between these results.

Figure 8 present the phasors-diagram at fixed voltage  $U_A=260 \text{ V}$ ; the numerical values of these phasors are:  $\underline{U}_B = -47,3 + j 358,1$ ;  $\underline{U}_C = 307,3 - j 358,1$ ;  $\underline{I}'_{a0} = 1,09 + j 1,65$ ;  $\underline{I}'_{b0} = 1,09 - j 0,71$ ;  $\underline{I}_{A0} = -0,78 - j 5,16$ ;  $\underline{I}_{B0} = 1,18 + j 1,01$ ;  $\underline{I}_{T0} = 0,4 - j 4,15$ .

## 6. CONCLUSION

The presented model can be used at the non-linear analysis of the capacitor motor. By coupling the circuit model with the anisotropic field model their results an analytical model that takes into consideration the non-linearity of the magnetization characteristic of the machine and the cross-saturation effect.

This coupled field-circuit model has been validated on a capacitor motor, on no-load with and without rotor cage; there have been good correlations between the computed and the measured values.

The proposed model is practical and flexible and it might be a starting base to the elaboration of a similar model for another type of elliptical field motor.

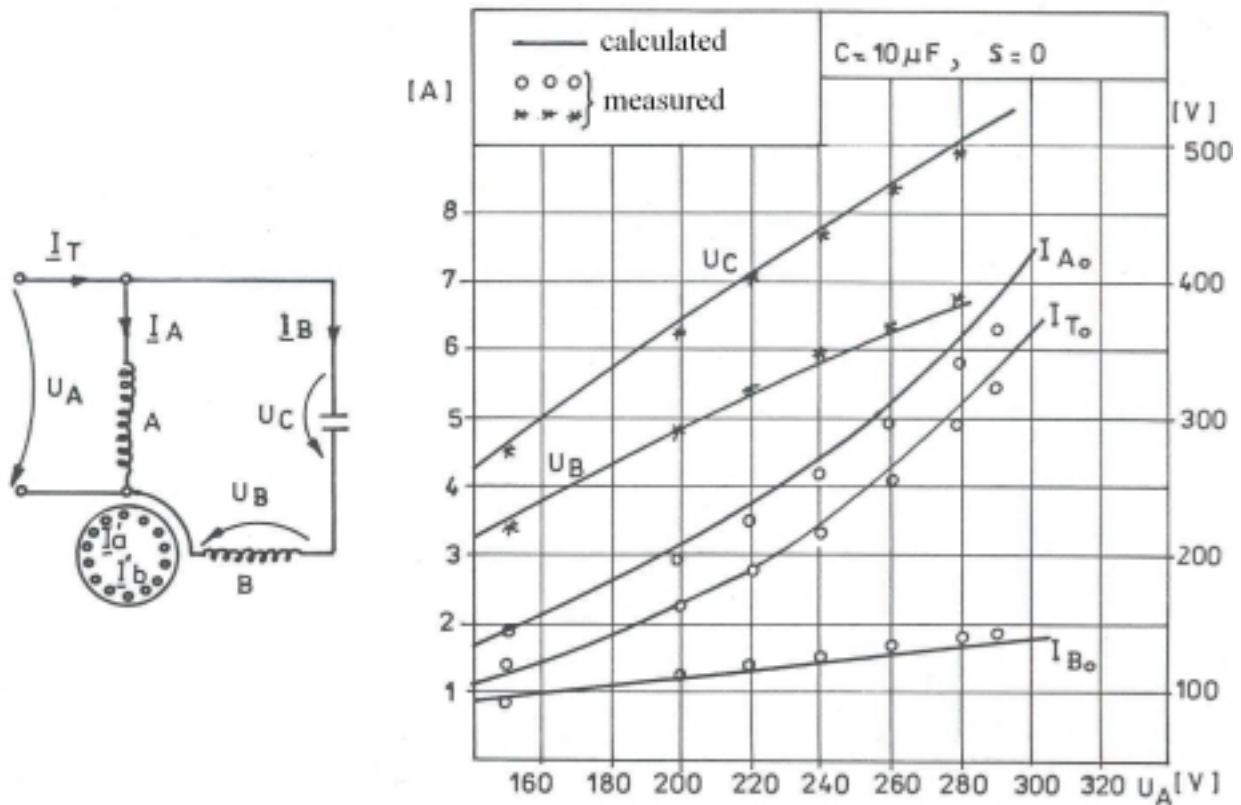


Fig. 7. The calculated and measured no-load currents and voltages for different values of  $U_A$  – voltage

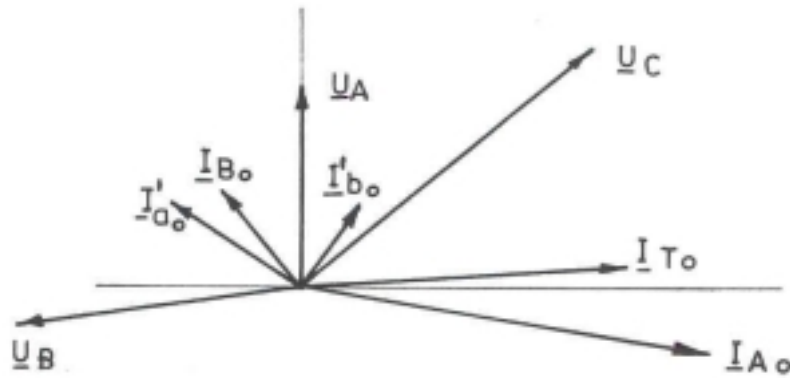


Fig. 8. The phasors- diagram for  $U_A = 260$  V

## REFERENCES

1. W.J. MORRILL, "Revolving-Field Theory of the Capacitor Motor", *Transaction on AIEE*, vol. 48, 1929, pp.614-628.
2. C.G. VEINOTT, *Theory and Design of Small Induction Motors*, McGraw-Hill Book Company, New York, 1959.
3. J. STEPINA, *Die Einphasen asynchronmotoren. Aufbau, Theorie und Berechnung*, Springer-Verlag Wien, New York, 1982.
4. T. DORDEA, *Mașini electrice. Teorie*, Editura ASAB, București, 2002.
5. I. BOLDEA, S.A. NASAR, T. DUMITRESCU, "Unified Analysis of 1-Phase AC Motors Having Capacitors in Auxiliary Windings", *IEEE Transaction on Energy Conversion*, vol. 14, no.3, sept.1999, pp. 577-582.
6. S.WILLIAMSON, A.C.SMITH, "A Unified Approach to the Analysis of Single-Phase Induction Motor", in *Proceedings of IEEE-IAS 1998 Annual Meeting*, vol.1, pp.87-94.
7. G.MADESCU, *Model neliniar al mașinii de inducție adaptat problemelor de optimizare*, Teză de doctorat, Universitatea „Politehnica” din Timișoara, 1996.

8. W.BURLIKOWSKI, K.KLUSZCZYNSKI, D.SZYMANSKI, "Determination of pulsating parasitic torques in a squirrel cage induction motor employing anisotropic machine model", in *Proceedings of ICEM 2000*, Helsinki, Finland, pp. 299-303.
9. A. MORARU, M. COVRIG, A. PANAITESCU, "The sinusoidal steady state induction machine. A field based approach. I: Theory", *Revue Roumaine des Sciences Techniques–Serie Electrotechnique et Energetique* Bucharest, 1996, 41,1, pp.3-12.
10. A. MORARU, M. COVRIG, A. PANAITESCU, "The sinusoidal steady state induction machine. A field based approach. II: Analytical and numerical solution", *Revue Roumaine des Sciences Techniques–Serie Electrotechnique et Energetique* Bucharest, 1996, 41,2, pp.155-167.
11. I.P.KOPYLOV, *Mathematical Models of Electrical Machines*, Mir Publishers, Moscow, 1984.
12. C.V.JONES, *The Unified theory of Electrical Machines*, London, Butterworths, 1967

*Received February 21, 2005*